Metal-to-DNA Base-Pair Ratios and Fluorescence Intensity of Silver Nanocluster-Capped Duplex DNAs

Hector Henry Oyem[1,2]* and Ifeanyi Mirian Oyem[3]

[1]*School of Chemistry, Newcastle University, United Kingdom.*
[2]*Department of Chemical Sciences, University of Delta, Agbor, Delta State, Nigeria.*
[3]*Department of Biological Sciences, University of Delta, Agbor, Delta State, Nigeria.*

ABSTRACT

The emission properties of silver nanoclusters stabilised by duplex DNA at varying Ag:DNA base-pair ratios were systematically investigated. Guanine and cytosine nucleobases are known to enhance the fluorescence of metal nanoclusters. Although extensive research has examined metal-DNA nanoclusters, reports standardising metal-to-DNA base-pair ratios to determine optimal fluorescence conditions remain scarce. This study offers mechanistic insights into the roles of metal ions and stabilising DNA concentrations in optimising the fluorescence of metal-DNA nanoconjugates. Five concentrations of Ag^+ ions were reacted with either one or two DNA base-pair concentrations and subsequently reduced with equimolar sodium borohydride under ambient conditions. The results revealed distinct variations in fluorescence intensity across different Ag:DNA ratios. Nanoclusters templated on two DNA base pairs exhibited stronger luminescence than those templated on a single base pair. The highest intensity was observed for the 0.5:2 and 3.0:2 Ag:DNA base-pair ratios for Ag:ctDNA and Ag:pdG-dCDNA, respectively. Average emission intensities were higher for pdC-dGAgNCs than for ctDNAAgNCs samples. All samples emitted near 430 nm, but with varied intensities. Contrary to expectations of a steady increase in emission intensity with increasing Ag^+ ion concentrations, the emission intensity followed a non-linear, random pattern. No consistent increases in emission values were observed with increasing Ag^+ ion concentration and DNA base-pair ratios. These findings underscore the importance of standardising Ag:DNA concentration ratios in fluorescence-based experiments, particularly for life sciences applications.

KEYWORDS

guanine, cytosine, fluorescence enhancement, delocalisation, resonance stability

Received: 7 October 2025 Revised: 24 April 2026 Accepted: 17 May 2026

INTRODUCTION

Fluorescence is a powerful analytical tool with broad applications in the physical and life sciences. It plays a critical role in optoelectronics, sensing, and bioimaging for detection and diagnosis.[1–3] Fluorescence occurs when certain materials absorb photons of light energy, causing excitation of electrons in the lower energy states to transit across the bandgap into a higher energy level, where it undergoes vibrational relaxation before returning to the ground state by releasing its excess energy as light.[4–6]

Nanoparticles are sub-microscopic materials with dimensions in the nanometer scale.[7–9] At this size scale, they exhibit quantum confinement effects and are therefore often described as 'particles' with molecular-like properties.[10,11] Their wavefunctions are confined,[12,13] and their properties are determined by the number of atoms they contain, which defines their density of states. Nanoclusters, a subclass of nanoparticles with relatively fewer atoms,[14] possessing a low density of states and discrete electronic energy levels.[15,16] This enables electronic transitions and fluorescence, unlike larger nanoparticles that exhibit continuous energy bands (no bandgaps) and typically do not fluoresce.[16]

However, nanoclusters' fluorescence is often short-lived because they tend to self-assemble into larger nanoparticles to achieve thermodynamic stability.[17–19] As a result, nanoclusters lose their discrete bandgaps and fluorescence. To prevent this, stabilising ligands such as DNA are used to cap nanoclusters. DNA nucleobases offer multiple binding sites for metal ions, forming base–metal–base bridge structures after reduction.[20,21] This conjugation restricts cluster aggregation and preserves their nanoscale properties.

Dickson and co-workers pioneered the study of metal-DNA templated nanoclusters in 2004.[22] Since then, numerous researchers have gone on to study various metal-DNA nano-conjugates using varied metal: DNA base (pair) ratios for oligonucleotides and duplexes, respectively [23,24] with incontrovertible evidence confirming this bio-nano-conjugation and properties of the DNA-Metal nanoclusters, using UV-Vis, fluorescence, NMR tools, and particularly electrospray ionisation mass spectroscopy (ESI-MS) to confirm the products.[22,25,26]

Among DNA bases, guanine- and cytosine-rich sequences are particularly effective at enhancing the fluorescence of metal nanoclusters (MNCs). Studies have consistently shown that guanine and cytosine (GC) -rich oligonucleotides generate stronger fluorescence than thymine- or adenine-rich sequences.[27–29] Consequently, synthetic GC-rich DNAs have widely been adopted as a stabilising ligand for nanoclusters.[30–34] Enhanced fluorescence is especially important in life science imaging, where intensity directly impacts image quality. Nonetheless, fluorescence in aqueous solution is often compromised by oxidation of Ag^0 to Ag_2O.

Calf thymus DNA (ctDNA), which contains a natural mix of nucleobases, offers limited control over the GC content. Whereas, polydeoxycytidine and polydeoxyguanosine (pdC – dG) synthetic block duplex DNA provides a direct basis for enriching DNA duplex with GC content; thus, establishing a direct contrast to ctDNA. Ag^+ ions acting as electrophiles favourably coordinate with the N3 and N7 positions of guanine and cytosine, resulting in extensive delocalisation of π-electrons across their heteroaromatic rings.[35,36] This delocalisation enhances resonance stability in all the DNA nucleobases, more so in cytosine and guanine, in contrast to adenine and thymine. Thereby contributing to the stability and hence fluorescence optimisation of the eventual DNA-metal nanoconjugates. [36]

In all the studies on metal-DNA stabilised nanoclusters, what is obvious is the absence of a standardised metal: DNA base ratio, irrespective of whether it was single- or double-stranded DNA molecules that were used. Efforts were rather largely centred on the

*To whom correspondence should be addressed
Email: hector.oyem@unidel.edu.ng

ISSN 1996-840X Online / South African Chemical Institute / http://saci.co.za/journal
© The Author(s) Published under a Creative Commons Attribution 4.0 International Licence (CC BY 4.0)
https://doi.org/10.17159/0379-4350/2026/v80se1a15

type of the DNA base sequences, with preference given to cytosine and guanine-rich sequences having been discovered to produce fluorescence enhancement.[27–29] Hardly has there been any deliberate attempt to standardise the metal:DNA base ratio, whether for single- or double-stranded DNAs. Instead, there is this random application or direct adoption of previously published metal: DNA base ratios of earlier researchers like Dickson. Building on these findings, the specific objective was to determine the appropriate Ag:DNA base-pair (bp) ratios that should produce optimum fluorescence using (ctDNA) and pdC-dG duplex DNAs. Thereby, providing a standardised analytical basis for deciding the appropriate reaction concentrations in metal-to-DNA-based research.

EXPERIMENTAL

Materials

Silver nitrate ($AgNO_3$, 99.0%), sodium borohydride ($NaBH_4$, 99.0%), polydeoxyguanosine–polydeoxycytidine (pdG–pdC) block duplex DNA, and calf thymus DNA, all from Sigma Aldrich, USA, were used without further purification. Deionised water was obtained from the Barnstead Millipore Diamond Series 170 (Model D11931, Barnstead International, Iowa, USA) and had a resistivity of 18.2 MΩ·cm.

Instrumentation

UV-visible absorbance spectra were recorded on a Varian 100 Bio spectrophotometer (California, USA) equipped with a deuterium arc lamp for the UV region and a tungsten halogen lamp for the visible region. Detection was carried out using an R928 photomultiplier tube (PMT) with a scanning range of 190–900 nm. Fluorescence spectra were obtained with a SPEX FluoroMax spectrofluorimeter (New Jersey, USA), fitted with an ozone-free xenon lamp as the excitation source, a photomultiplier detector for emission, and a photodiode reference detector. The instrument operated over an excitation/emission wavelength range of 200–950 nm and was optimised for the UV–visible region. Both instruments operated at 220 V, and all measurements were performed at room temperature using a 500 µL quartz microcuvette (Hellma UK Ltd).

Preparation of Stock solutions

Standard solutions of $AgNO_3$ and $NaBH_4$ were prepared by weighing 0.1700 g and 0.0378 g of the salts, respectively, into clean 5 mL glass vials and dissolving them in 1 mL of Nanopure deionised water to obtain 1 M solutions. From these, 10 µL portions were withdrawn using a micropipette into separate 10 mL volumetric flasks and brought up to the mark with deionised water to obtain 1 mM $AgNO_3$ and $NaBH_4$ aqueous stock solutions.

Stock solutions of ctDNA and pdC-dGDNA were prepared by weighing 1 g of each sample into 1 mL Eppendorf tubes and dissolving in 1 mL of deionised water. Then, 10 µL aliquots were transferred into a clean microcuvette and filled to the mark with deionised water. The sample concentrations were subsequently determined spectroscopically by UV-Vis spectrophotometer. The molar concentration was obtained by dividing the concentration in µg/mL by a conversion factor of 494.5, which is the molar mass of a base pair. We then multiplied these molar concentrations by the dilution factor of 100 to obtain the concentration for each of the 1 mL DNA samples.

Preparation of Ag^+: DNA Ratios and Reaction Synthesis

With a fixed DNA concentration of 5×10^{-6} M for all DNA samples, the required concentrations of the $AgNO_3$ solution containing Ag^+ ions to bind onto the DNA molecules were calculated from the individual concentration ratios. For example, 0.5:1 bp corresponds to 2.50×10^{-6} M of Ag^+, while 0.5:2 bps gives 1.25×10^{-6} M of Ag^+.

Five concentration ratios of Ag^+ to DNA base pairs (0.5:1, 1.0:1, 1.5:1, 2.0:1, and 3.0:1 for one bp) and another five corresponding to 0.5:2, 1.0:2, 1.5:2, 2.0:2, and 3.0:2 for two bps were prepared by mixing appropriate aliquots of DNA and $AgNO_3$ solutions. For clarity, these concentration ratios are now labelled: (a, b, c, d, and e) and (2a, 2b, 2c, 2d, and 2e) respectively for the various concentrations of Ag^+ to one and two DNA bp(s). These mixtures were then reduced with equimolar portions of $NaBH_4$ in a 1:1 mole ratio with the $AgNO_3$ solution, before the samples were incubated in the dark at room temperature for 30 minutes.

Similarly, the Ag^+:DNA ratio denotes the concentration of Ag^+ ion relative to DNA concentration. For instance, a 0.5:1 DNA ratio connotes an Ag^+:concentration of 0.5 to 1 or 2 DNA bp(s). Meanwhile, the notation: bp, which represents base pair, is ascribed to one base pair; whereas, bps implies more than one base pair (e.g. two base pairs). A base pair describes two DNA bases, and two base pairs comprise the full four complements of DNA bases.

Spectroscopic Analyses

Absorbance and fluorescence spectra were recorded for each sample immediately afterwards by taking 10 µL of each sample and adding deionised water to bring it up to the mark. The samples were then placed in UV-Vis and fluorescence spectrophotometers, and their absorbance and emission data were obtained by scanning across the wavelength range of 200 – 800 nm. Control experiments comprised DNA samples (only) as the negative control and, obviously, aggregated silver nanoparticles (Ag NPs) (without DNA) as the positive control sample. All control samples were prepared under the same experimental conditions as the analyte samples for comparison.

RESULTS AND DISCUSSION

The results of the spectroscopic analyses of the samples are presented below:

Absorbance

The absorbance (ABS) spectra of all the Ag: DNA nanoconjugates in Figure 1 show a noticeable decrease of the original DNA peak at 260 nm when contrasted with the same DNA peak of the pure DNA sample (control). This observation is taken as an early indication of the successful binding of Ag to DNA molecules. Metal ions variously bind to the nitrogen-containing nucleobases in the DNA molecules.[20,36,37]

In all, the ABS spectra of both sets of experiments do not show any presence of the usual local surface plasmon resonance (LSPR) associated with silver nanoparticles (Ag NPs) that usually indicates the presence of large non-fluorescent Ag NPs often seen around 400 – 430 nm in the UV-Vis spectra of samples of Ag NPs.

This observation is of crucial analytical significance, since we are particularly interested in synthesising fluorescent silver nanoclusters (Ag NCs) that are much smaller and possess the requisite bandgaps necessary for electronic transitions, and consequently result in fluorescence emissions.[36] The production of Ag NCs rather than Ag NPs is the intrinsic intention of this experimental design. This is because Ag NPs are already too big in terms of their density of state and as such do not possess the requisite electronic bandgaps necessary for electronic transitions between energy levels.[38] Low density of state is a characteristic of ultra-small NPs, better referred to as NCs. These often contain between 2 – 20 atoms with a diameter not exceeding 2 nm; they possess unique molecule-like opto-physical properties.[39] NCs are noted for having distinct electronic bandgaps which are significant for electronic transitions.[40]

Besides the use of particle-size analysers, nanoscientists can readily foretell the size of the particles from studying the UV-Vis and emission spectra of the samples. Larger NPs often produce distinct LSPR in the UV-Vis spectrum of their samples.[41,42] This depicts the valence electrons resonating at a particular frequency of the electromagnetic

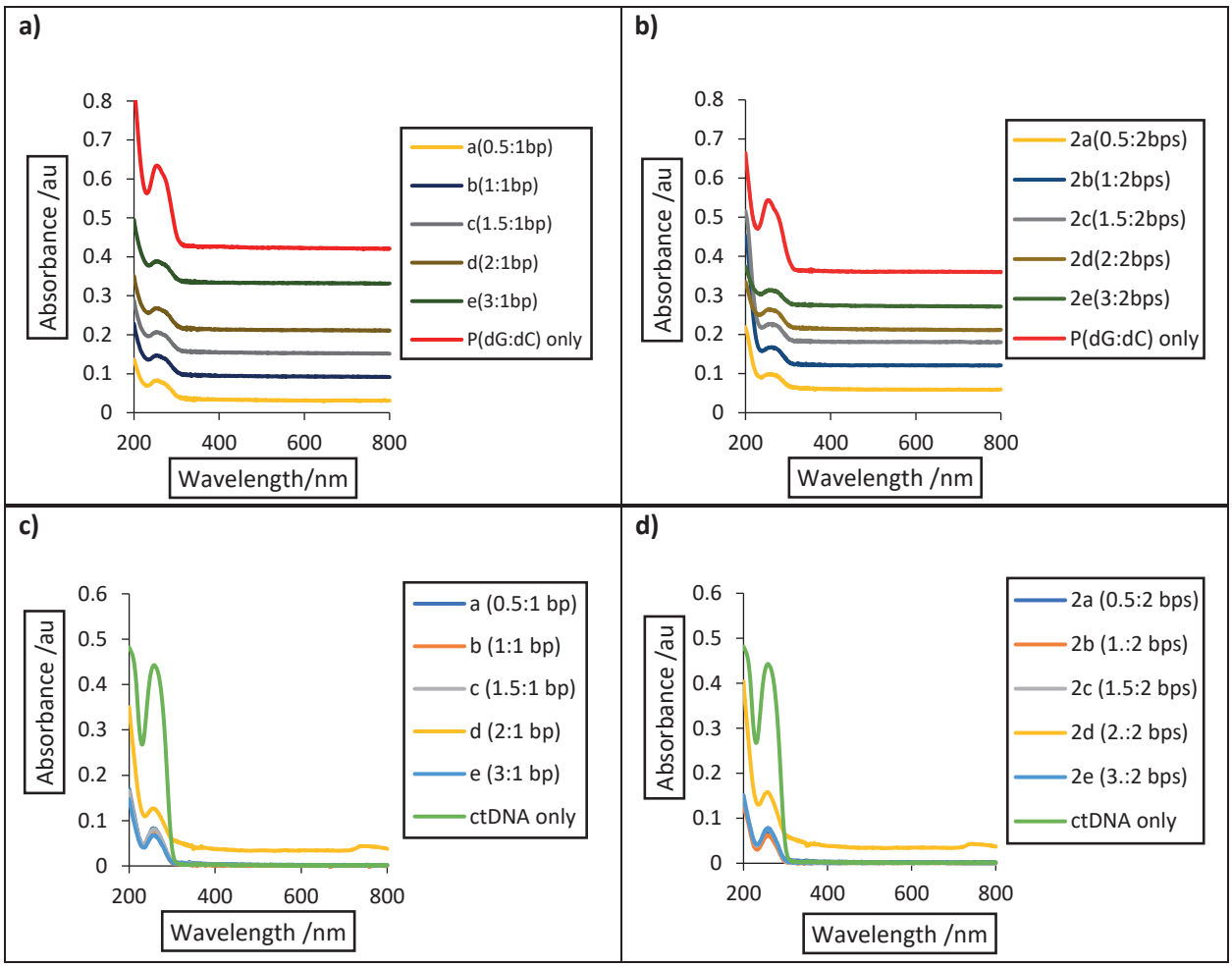


Figure 1: Absorption spectra of the Ag NC:pdG-dCDNA concentration ratios for: **a)** 1 bp, and **b)** 2 bps Ag NC:pdG-dCDNA base; **c)** 1 bp, and **d)** 2 bps AgNCs:ctDNA. Figures contain stacked absorbance spectra of the different AgNC:pdG-dCDNA and AgNCs:ctDNA concentration ratios for clearer observation; absorbance values are arbitrary units (au).

radiation.[42] Ag NPs have an established LSPR band appearing between 400 – 430 nm wavelength.[41,43,44] Contrastingly, Ag NCs show no such LSPR bands in their UV-Vis spectra. This is because, unlike the Ag NPs, where the electronic energy levels are already occupied (higher density of state), therefore preventing electronic transition, the NCs have no such limitation. Instead, electronic transitions occur by excitation, resulting eventually in emission as the exciton returns to the 'hole' in the ground state.[45] This observation appears clearly in the fluorescence spectra (FLS) of the Ag NCs but is obviously absent in the FLS of the Ag NPs. Apparently, these notable disparity in electronic spectra is often an early indication of the presence or absence of Ag NPs or Ag NCs in the as-synthesised samples.

Accordingly, the absorbance results obtained align with the objectives and conceptual framework of this research, which is to produce Ag nanoclusters (Ag NCs) that are luminescent upon interaction with electromagnetic radiation. The DNA template stabilises and restricts the growth of Ag NCs, preventing their aggregation into non-luminescent Ag nanoparticles (Ag NPs), which would otherwise result from spontaneous growth by aggregation, known as Ostwald ripening. [46,47]

Apart from the ostensible DNA bands usually at 260 nm, all spectra of the samples presented in Figures 1(a-d) show no discernible LSPR bands at 400 – 430 nm, which is the usual signature of the presence of Ag NPs.[41,48] Furthermore, this is also a diagnostic inference showing that the DNAs are effective at stabilising the Ag NCs from aggregating and forming the rather non-luminescent Ag NPs, which are clearly not the target products of these reactions.

Fluorescence

Ag NCs-pdC-dG DNA

Generally, the fluorescence emission spectra of the samples in this study are poor in terms of intensity output, as can be seen in the values of their fluorescence emission counts per second (cps). These can be observed in the spectra presented in Figures 2, 3, 4 and 5. Fluorescence outputs in aqueous solutions of DNA-nanoclusters are often bogged down by the problem of oxidation, as this depletes the stock of Ag NCs, thereby requiring some researchers to undertake this synthesis in the atmosphere of an inert gas like argon.[49] Furthermore, the structure of the duplex DNA portends a steric hindrance for electrophiles reaching the site of the nucleobases. These are considered to be factors which are thought to be responsible for the poor fluorescence output. Nevertheless, the main reason for the low intensity of the fluorescence outputs of these samples is believed to be connected to the proportion of the samples taken for analysis. In all, 10 µL each of the samples was pipetted into a micro cuvette with an approximate volume of 500 µL (0.5 mL) and made up to the mark with deionised water; thus, translating to a dilution factor of 50. The intention was to prevent the inner filter effect in our readings.

Regardless, the key point here is that the fluorescence intensities obtained varied with metal:DNA base pair (M:DNA bp) ratios. The most intense fluorescence peak for the Ag:pdG-dCDNA was provided by the Ag:DNA bp ratio of 1.0: 1 bp (corresponding to b) for the Ag:1 bp concentration ratio. The order of fluorescence intensities for these samples was: b > e > c > a > d, respectively (Figure 2).

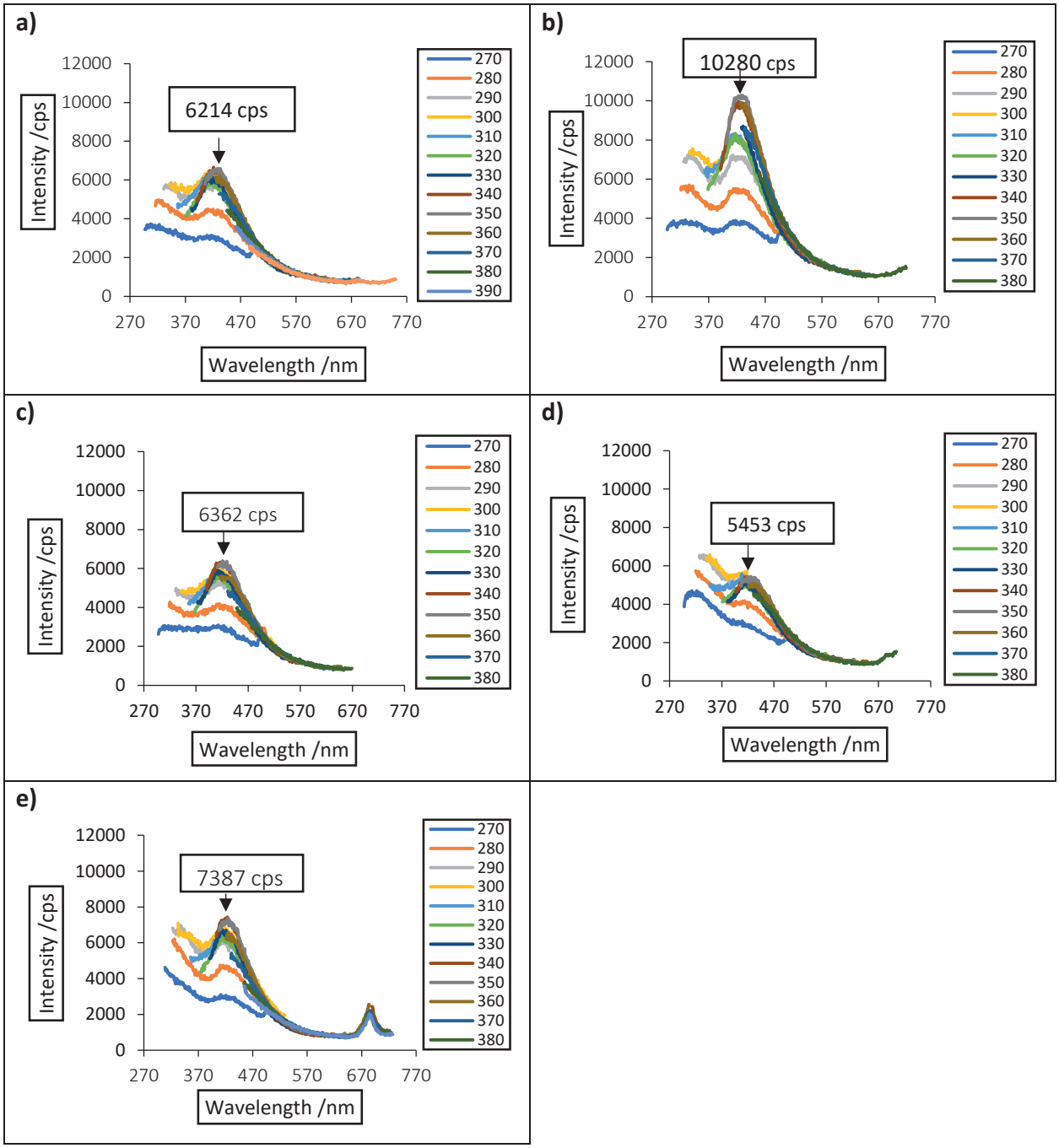


Figure 2: Emission intensities of Ag NCs templated on pdG-dCDNA at different Ag:pdG-dCDNA base pair concentration ratios: a) 0.5:1 bp, b) 1.0:1 bp, c) 1.5:1 bp, d) 2.0:1 bp, and e) 3.0: 1 bp.

The obvious variations in the fluorescence intensities of the different Ag:DNA bp ratios give credence to the need to standardise metal:DNA bp ratios in fluorescence.

Meanwhile, Figure 3 contains the fluorescence outputs of different Ag:2DNA bps concentration ratios. Comparing this with Figure 2 reveals an improvement in the emission intensities of Ag:2 DNA bps against those of Ag: 1 DNA bp in Figure 2. This is indicated by the values of the number of cps recorded in both of these spectra. This leads to the conclusion that Ag coordinated to 2 bps produced more stable nano-compounds.

In all, the highest fluorescence intensity was obtained from the 3.0: 2 bps (that is, 2e) Ag: DNA bps ratio with a fluorescence count of 13 x 10^3 cps. The 0.5: 2 bps (that is, 2a) Ag:DNA bps ratio produced the second highest fluorescence intensity at close to 11 x 10^3 cps. The fluorescence intensities of the five samples in Figure 3 followed the following order: 2e > 2a > 2b > 2d > 2c.

Ag NCs:ctDNA

Results of the Ag:ctDNA concentration-dependent fluorescence emission intensity study are displayed in Figures 4 and 5 for Ag^+:ctDNA 1bp and Ag^+:ctDNA 2 bps reduced with $NaBH_4$. From both figures, it is immediately obvious that there are three emission bands in most cases, although the third band, which is usually weak, is either absent or nearly absent in a few of these spectra. The three bands in the spectra occur at approximately 340, 430, and 680 nm, respectively, with excitation energies in the 280 – 360 nm range. The first two bands on the blue portion of the visible region of the electromagnetic spectrum (EMS) are considered to comprise of small clusters of Ag according to the region of light where these emission bands occur. These emissions translate to clusters with large bandgaps of approximately 2.86 eV for the 430 nm emission. The fluorescence characteristics of Ag NCs are intricately associated with their size and structure. Size-dependent changes in NCs alter the fluorescence

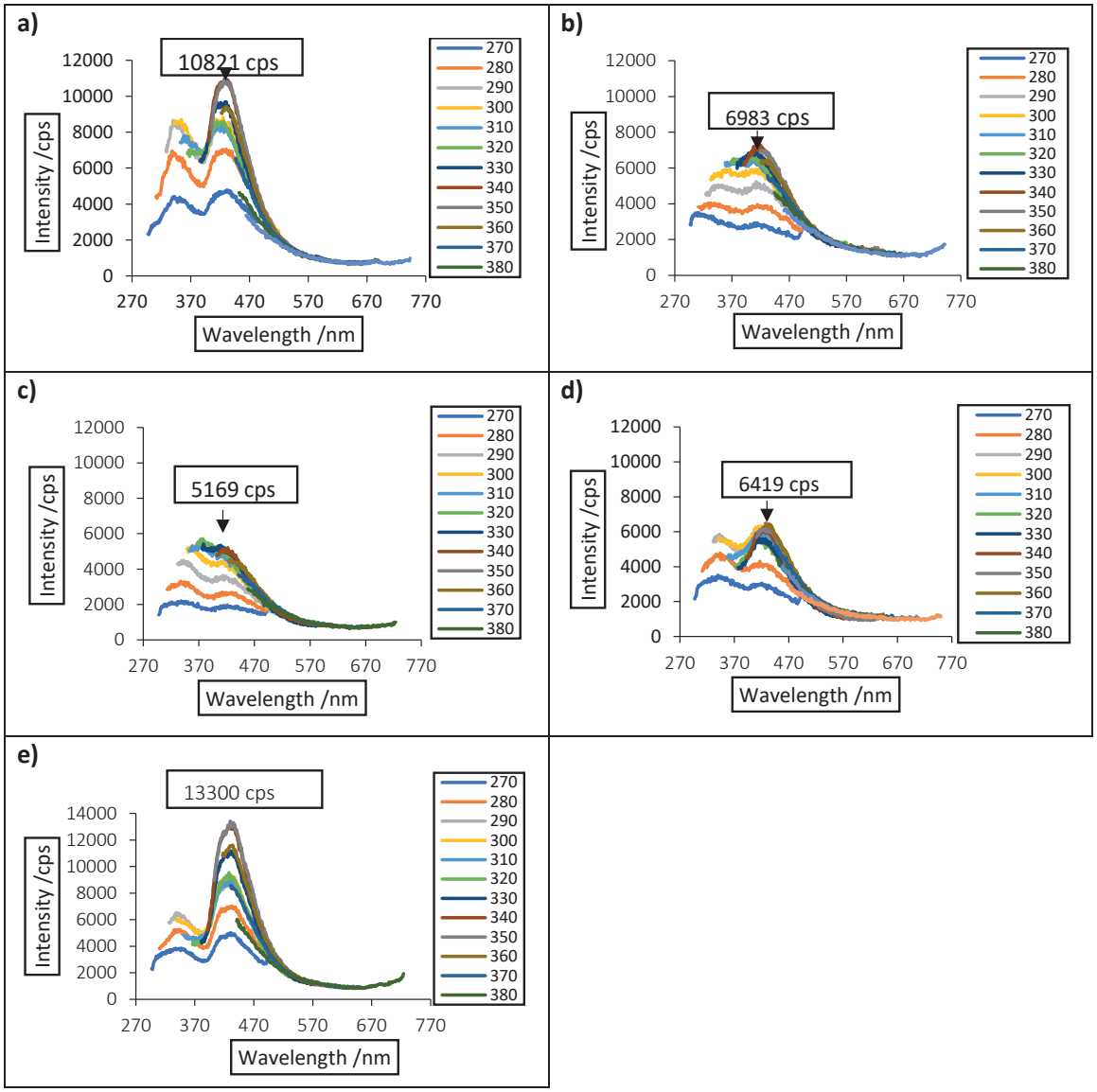


Figure 3: Emission intensities of Ag NCs template on pdG-dCDNA at different Ag^+:pdG-dCDNA base pair concentration ratios: a) 0.5: 2 bps, b) 1.0: 2 bps, c) 1.5: 2 bps, d) 2.0: 2 bps, and e) 3.0: 2 bps.

emission wavelength, a phenomenon known as size-dependent fluorescence.[50] Large bandgaps are characteristic of ultra-small NCs.[51] The region of the 430 nm emission band is in the blue region of the UV-Vis spectrum of the EMS; this is a signature of small NCs typically referred to as blue-emitters. [52–54]

While excitation wavelengths indicate the wavelength and energy equivalent absorbed and leading to electronic transition into higher energy levels, the value of the wavelength of the emission maximum, on the other hand, reflects the value of the energy difference (bandgap) (in electron volt, eV) between the ground state and the excited state. That is, the highest occupied molecular orbital and the lowest unoccupied molecular orbital (HOMO – LUMO).[5,26,40,55] Hence, scientists can estimate this energy difference – bandgap – from emission data. Consequently, Buceta and coworker[56] leveraging on emission data, proposed a simple equation which relates cluster size to emission wavelength. Thus, converting wavelength to eV to approximate the cluster size (number of atoms, N) of Ag NCs, from Equation (1) below:

$$N = \left(\frac{E_F}{E_g}\right)^3 \quad (1)$$

Here E_F is the Fermi level (5.4 eV for bulk Ag), and E_g is the HOMO–LUMO energy bandgap in eV.

Meanwhile, red-shifted emissions typify metal-to-ligand energy transfer corresponding to smaller bandgaps as can be observed for the 680 nm emission, translating to a bandgap of 1.96 eV. However, the first emission bands in all of the spectra in this study have been assigned to the d – d transitions of clusters of $Ag_4^{2+}{}_{(aq.)}$. The origin and significance of this band are associated with the onset of cluster formation.[57] Further details will be given in the following section.

Although the fluorescence intensities of the samples were again characteristically low, the significance of varying the Ag:DNA bps ratio on the eventual fluorescence intensity of the resulting Ag-DNA nanoconjugates is not in doubt. Invariably, it goes without saying, particularly in the areas of sensing and imaging science, where fluorescence quantum yield and intensity are crucial, and optimum fluorescence is ideal, that the best metal:DNA bp concentration ratio would be required and generally adopted.

To this extent, our experiments justify the adoption and application of the ideal metal: DNA base pairs ratios in fluorescence experiments. These results are unanimous in demonstrating the connection between metal:DNA bp ratios and fluorescence intensities of metal nanoclusters-DNA (MNCs- DNA) conjugates. However, there are no silver bullets, that is to say, there is no particular Ag: DNA bp(s) ratio which cuts across all spectrum of DNA types. In other words, the optimum Ag: DNA bp(s) concentration ratio depends on the type

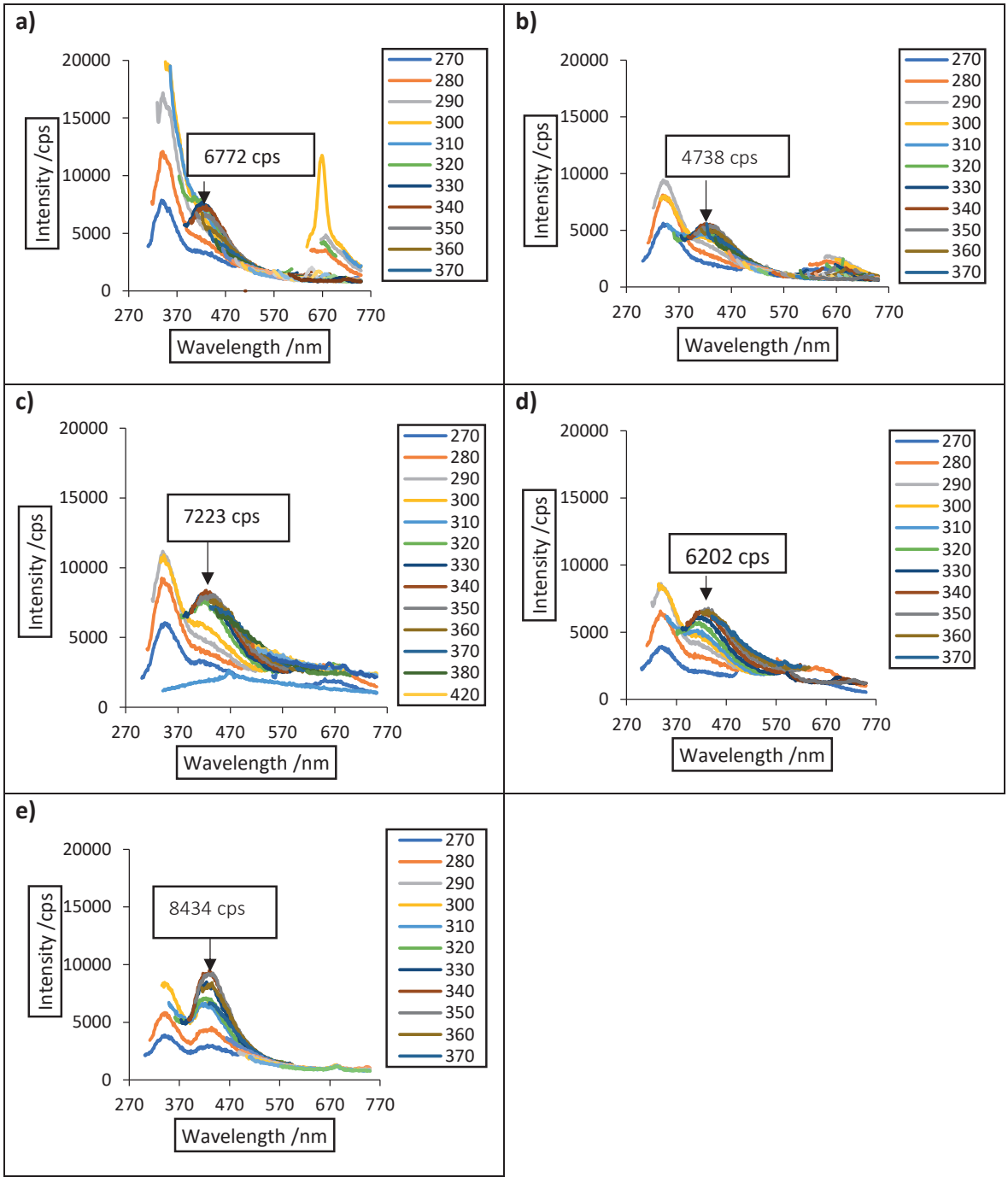


Figure 4: Emission intensities of Ag NCs templated on ctDNA at different Ag^+:ctDNA base pair concentration ratios: a) 0.5:1 bp, b) 1.0:1 bp, c) 1.5:1 bp, d) 2.0:1 bp, and e) 3.0: 1 bp.

of DNA ligand employed in these experiments. Therefore, optimum Ag:DNA bp(s) should be determined experimentally through a standardisation process.

All the spectra in Figures 2, 3, 4 & 5 show basically two emission bands at 350 and 430 nm. The former is ascribed to d – d transitions of $Ag_4^{2+}{}_{(aq.)}$. These bands are clear markers connoting the onset of the formation of Ag NCs during the process known as the nucleation stage of nanocluster formation;[26,58,59], while the latter band is attributed to the Ag NCs $(Ag^0)_n$, which are the products of the nucleation process.[22] Consequently, the intensity of the 350 nm band steadily decreases even as the 430 nm band increases concomitantly with Ag NCs formation. Similar trends of emission bands have been reported for Ag NCs in the literature.[26] In an earlier study by Oyem using ctDNA, these emission bands were observed, showing the formation of similar species of Ag NCs in these experiments.[60]

Meanwhile, an excitation wavelength of 340 nm was observed to be responsible for this 430 nm emission in all the samples. This signifies that the samples contained similar species of Ag NCs by size. The positions of NCs' emission bands are size-related – a shift towards the red end of the spectrum (longer wavelength) infers larger particle size and vice versa. That is why particles are often described as blue, green, yellow or red emitters in literature.[61]

On rare occasions, as previously stated, we also notice a small band at 680 nm, suggesting that such emission may have occurred as a result of energy transfer, as has been reported by Dickson and his coworkers.[57]

The variability of the emission intensity counts of both the pdG-dCDNA and the ctDNA templated Ag NCs with Ag^+:DNA bp concentration ratios highlight the need to predetermine the metal: DNA concentration ratio for better analytical sense. More so, if the essence of the experiment is to produce brightly fluorescing NCs

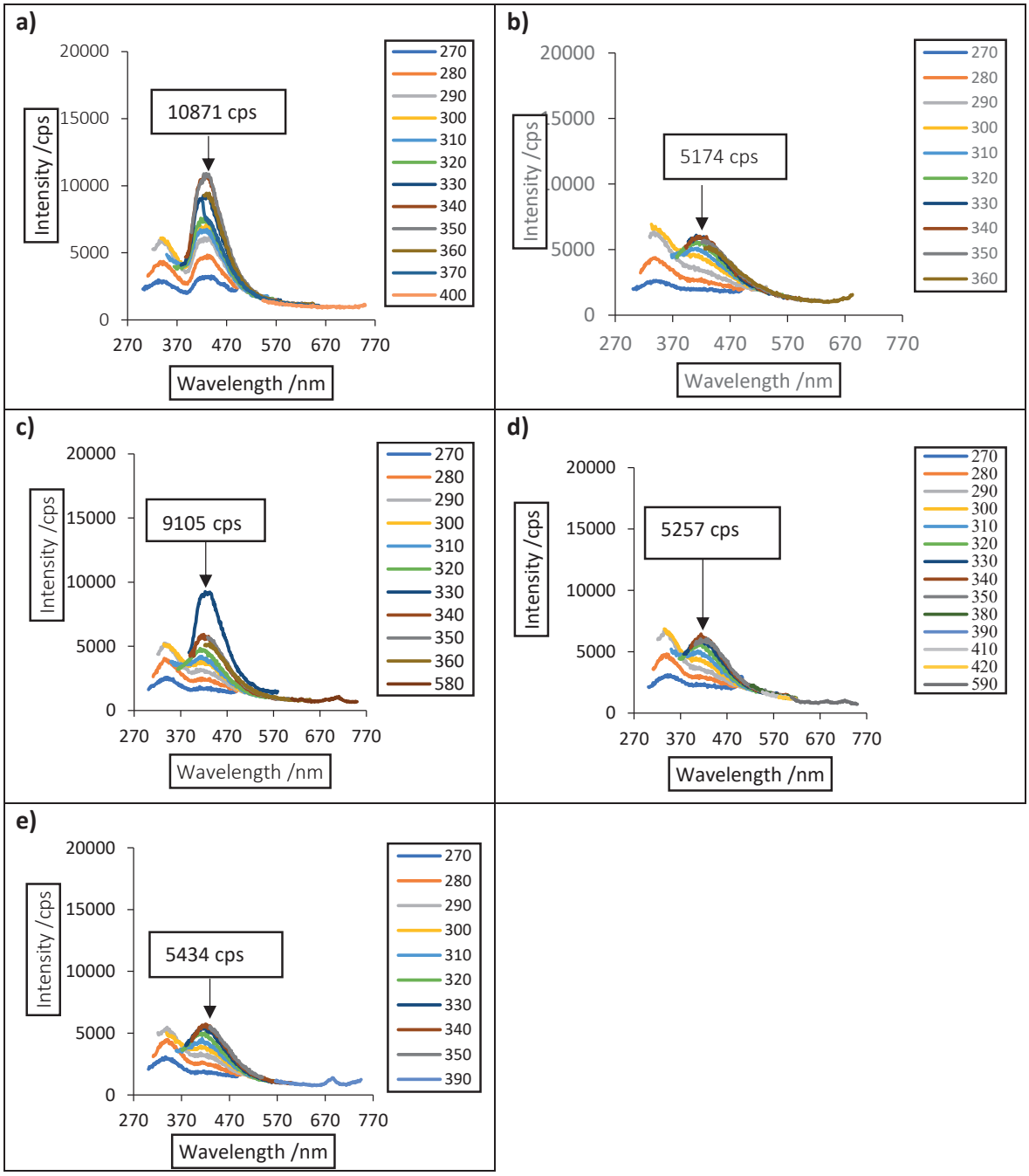


Figure 5: Emission intensities of Ag NCs template on ctDNA at different Ag^+:ctDNA base pair concentration ratios: a) 0.5:2 bps, b) 1.0:2 bps, c) 1.5:2 bps, d) 2.0:2 bps, and e) 3.0: 2 bps.

of optimum intensity, as would be the case in life sciences, where fluorescence imaging is ideal.

The conformation which gives the best stability and also the most concentration of Ag NCs on DNA scaffold is thought to result in a stable nanoconjugate and produce optimum luminescence – highest cps. Otherwise, their intensities should either remain constant (reflecting an indifference to Ag^+ concentration increases) or change linearly with increasing Ag^+ ion concentration per bp(s) and vice versa.

The main 430 nm Ag NCs-ctDNA emission band

Ostensibly, as the Ag^+ ion concentration increased, the emission intensity of the 430 nm emission band did not increase concomittantly (Figure 6). Even though the general indication according to the thread line in Figure 7 portends that the emission intensity followed the concentration of the Ag^+ ions. Although the observed variation in emission intensity in some of these samples is believed to indicate the apparent favourability for certain structural geometry with increasing metal:DNA base ratio, and the stability of the resulting nanoconjugate. A striking finding shows that the most intense emission was obtained with an Ag^+:ctDNA bp ratio of 3.0:1 bp. This signifies that for a bp, that is, two DNA bases, higher Ag^+ ion concentrations favoured more intense emissions. Therefore, the 3.0:1 bp ratio (labelled a), by interpretation, is the most efficient concentration ratio for Ag:DNA bp and hence produced the most optimal fluorescence intensity for that category.

Furthermore, in Figure 7b above, which contains a spectrum of increasing Ag^+ ion:2 bps, we see a complete reversal of the previous trends observed in Figure 7a. The general indication is that the emission intensity decreased with increasing Ag^+ ion concentration, albeit with two ctDNA bps; that is, four ctDNA bases. The highest emission intensity was produced by the 0.5:2 bps (2a) concentration ratio for this category of samples.

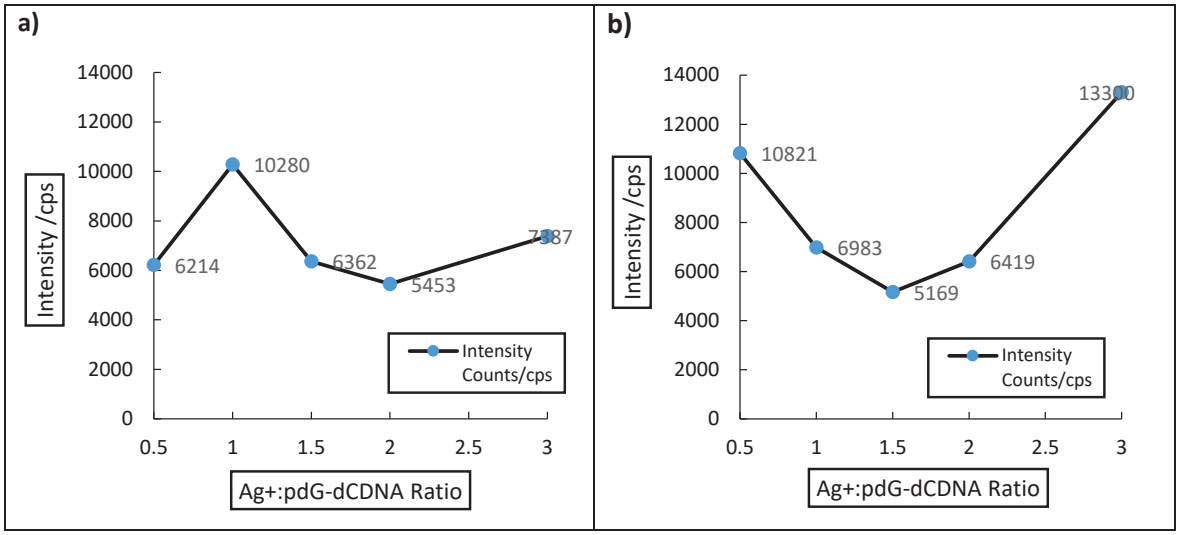


Figure 6: Emission intensity counts of pdG-dCDNA template Ag NCs (a) $Ag^{+:}1$ DNA base pair (b) $Ag^{+:}2$ DNA base pairs.

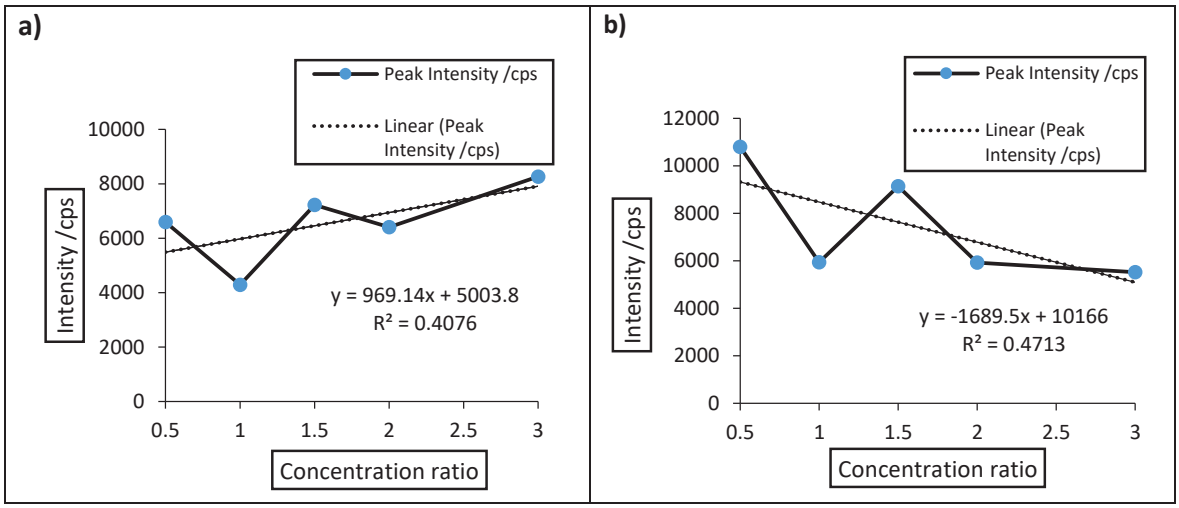


Figure 7: Chart of Ag^{+}:ctDNA bp(s) concentration ratios against the intensity of the 430 nm emission band: a) one base pair, and b) two bps.

The intensity of a fluorescence emission band is attributed to the concentration of the fluorophores, thus demonstrating that the 3.0:1 bp (e) in Figure 4, as well as the 0.5:2 bps (2a) concentrations in Figure 5, both yielding the most intense fluorescence for the Ag:ctDNA, are considered to have produced the highest concentration of Ag NCs fluorophores than any other in this study.

Fluorescence emission intensities followed the order: b > e > c > a > d, respectively, for Ag NCs conjugated onto one pdG-dCDNA bp (Figure 6); whereas Ag NCs that were bonded to two pdG-dCDNA bps recorded fluorescence intensity in the order:2e > 2a > 2b > 2d > 2c. It was e > c > a > d > b; and 2a > 2c > 2b > 2d and 2e for the Ag:ctDNA sample. Emission consistently occurred at ~430 nm, with variations in intensity rather than wavelength.

The most effective excitation wavelength for the 430 nm emission

The emission band at 430 nm appeared in all the samples of this study and is attributed to Ag NCs. This author observed a similar emission band at 430 nm in a recent study of Ag NCs stabilised by inorganic borate and borane ligands, being oxidation products from the $NaBH_4$ reducing agent in a water-in-oil microemulsion study.[57] This suggests that both the pdG-dCDNA and ctDNA ligands in this study are stabilising similar Ag NCs species. The 430 nm emission band was produced by the 340 nm excitation wavelength, considered to have provided the most effective excitation energy required for this prominent 430 nm emission. We can see the impact of this 340 nm wavelength excitation energy in the spectra of Figure 8.

Emission intensity varied with the Ag:DNA ratio for 1 bp. However, intensity generally remained roughly the same for Ag NCs templated on 2 bps, except for the 0.5:2 (2a) Ag:DNA ratio, suggesting an increase in the concentration of the Ag NCs that is emitting at this 430 nm wavelength. The uniqueness of this emission band may be associated with the conformational stability of the Ag:DNA conjugate at this particular concentration ratio (2a).

Undoubtedly, the appropriate metal:DNA bp(s) concentration ratio adopted in an experiment would obviously impact the intensity of the emission band of the resulting MNCs. It is therefore unreasonable to randomly adopt any concentration ratios for these types of experiments. Moreover, chemistry requires that reacting species combine stoichiometrically, that is, they react according to concentration mole ratios. One would therefore expect that nanoclusters' formation using DNA as a stabilising ligand would similarly follow some semblance of concentration-dependent stoichiometry. In this case, we have been able to demonstrate using duplex DNAs like calf thymus and pdC-dG block DNA that the appropriate metal: DNA ratio is crucial for optimal luminescence.

CONCLUSION

The effect of varying metal: DNA bp ratio on the emission intensity of Ag NCs was investigated for different combinations of Ag: DNA bp(s)

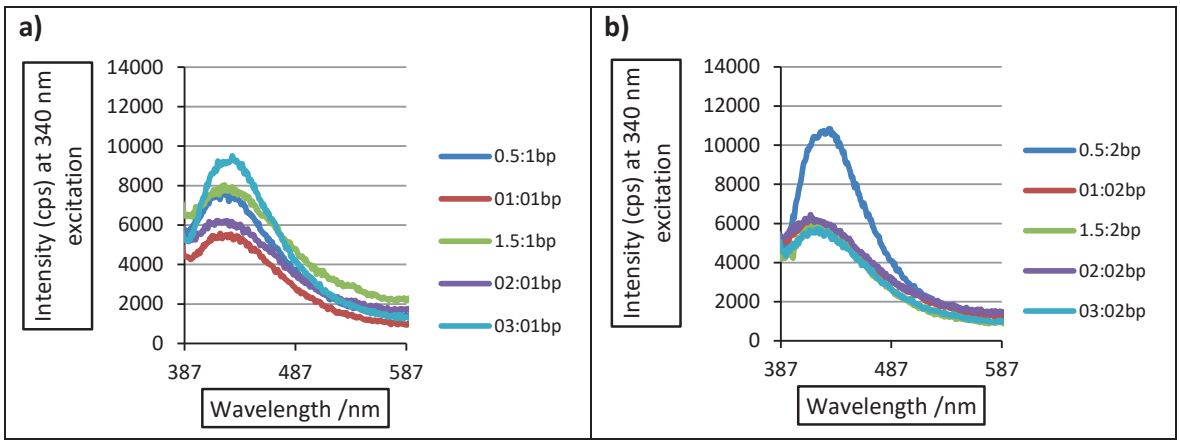


Figure 8: Fluorescence emission of different Ag:ctDNA concentration ratios at the optimum excitation wavelength of 340 nm for the emission band at 430 nm, for a) 1 base pair, and b) 2 base pairs respectively.

concentrations to determine the right metal:DNA bp ratio which produced the most luminescence using pdG-dCDNA and ctDNA as stabilising ligands. Fluorescence intensity serves both quantitative and qualitative purposes; high or low intensities depict the brightness or otherwise of a sample's luminosity, especially when viewed under UV-light. Findings show that, whereas all the samples have the same emission bands/wavelengths, metal:DNA base ratios seemingly affected the fluorescence emission intensities. Critically, there is a certain metal: DNA bp ratio that produced the most fluorescent efficiency.

Furthermore, the number of DNA bps involved in coordination with Ag^+ ions similarly affected the emission characteristics of the Ag NCs. On average, the emission intensities of the pdC-dGAgNCs were higher than the ctDNAAgNCs, giving credence to the famed GC-rich enhancement of fluorescence. Nanoclusters templated on two DNA bps exhibited stronger fluorescence than those on a single bp. The conformational stability of the metal:DNA nanoconjugate likely influenced the variability of fluorescence emission intensity. Evidence points to the existence of a metal:DNA base pair concentration ratio that provided optimal fluorescence with DNA-templated MNCs. These findings obviously highlight the importance of standardising Metal:DNA ratios in fluorescence-based experiments for sensing and bioimaging applications.

SUPPLEMENTARY INFORMATION

This manuscript does not have Supplementary Information. All the data is presented in the article.

ACKNOWLEDGEMENT

Acknowledgement is due to Newcastle University, United Kingdom and particularly the School of Chemistry, Chemical Nanoscience Laboratory, Bedson Building.

AUTHOR CONTRIBUTIONS

Hector Henry Oyem: The experimental measurement and analysis, as well as writing the original manuscript. Ifeanyi Mirian Oyem: Participated in the paper preparation and design, as well as the review and editing of the manuscript. She was also involved in addressing some comments from the reviewers.

DECLARATION OF COMPETING OR FINANCIAL INTERESTS

Authors declare no conflicting interests.

DECLARATION OF GENERATIVE AI AND AI-ASSISTED TECHNOLOGIES

The authors used Grammarly to grammar check the manuscript. Final revision and editing were done before submission.

AUTHORS ORCID

Hector Henry Oyem: https://orcid.org/0000-0003-4877-2221
Ifeanyi Mirian Oyem: https://orcid.org/0000-0002-5883-5030

REFERENCES

1. Fakayode SO, Lisse C, Medawala W, Brady PN, Bwambok DK, Anum D, Alonge T, Taylor ME, Baker GA, Mehari TF, Rodriguez JD, Elzey B, Siraj N, Macchi S, Le T, Forson M, Bashiru M, Narcisse VEF, Show CG. Fluorescent chemical sensors: applications in analytical, environmental, forensic, pharmaceutical, biological, and biomedical sample measurement, and clinical diagnosis. Appl Spectrosc Rev. 2023; 59: 1–89. https://doi.org/10.1080/05704928.2023.2177666
2. Lu P, Ai J. Fluorescence probes and their sensing applications in nanomaterial systems. Talanta Open. 2023; 8: 100248. https://doi.org/10.1016/j.talo.2023.100248
3. Mishra V, Razi SS, Kumar A. *Functional Fluorescent Materials: Applications in Sensing, Bioimaging, and Optoelectronics*. 1st ed. CRC Press: Boca Raton, Florida, 2024 https://doi.org/10.1201/9781003352372
4. Adewuyi A, Lau WJ. Chapter 3 - Nanomaterial development and its applications for emerging pollutant removal in water. In: Lau WJ, Faungnawakij K, Piyachomkwan K, Ruktanonchai UR (eds). Micro and Nano Technologies, Handbook of Nanotechnology Applications. Elsevier. 2021; 67–97. https://doi.org/10.1016/B978-0-12-821506-7.00003-X
5. Teunis MB, Dolai S, Sardar R. Effects of surface-passivating ligands and ultrasmall CdSe nanocrystal size on the delocalisation of exciton confinement. Langmuir. 2014; 30: 7851–7858. https://doi.org/10.1021/la501533t
6. Xie Y, Teunis BM, Pandit B, Sardar R, Liu J. Molecule-like CdSe Nanoclusters Passivated with Strongly Interacting Ligands: Energy Level Alignment and photoinduced Ultrafast Charge Transfer Processes. J Phys Chem C. 2015; 119: 2813–2821. https://doi.org/10.1021/jp510276c
7. Khan I, Saeed K, Khan I. Nanoparticles: Properties, applications and toxicities. Arab J Chem. 2019; 12: 908–931. https://doi.org/10.1016/j.arabjc.2017.05.011
8. Baig N, Kammakakam I, Falath W, Kammakakam I. Nanomaterials: A review of synthesis methods, properties, recent progress, and challenges. Mater Adv. 2021; 2: 1821–1871. https://doi.org/10.1039/d0ma00807a
9. Mekuye B, Abera B. Nanomaterials: An overview of synthesis, classification, characterisation, and applications. Nano Sel. 2023; 4: 486–501. https://doi.org/10.1002/nano.202300038Digital Object Identifier (DOI)
10. Khan S, Hossain MK. Classification and properties of nanoparticles. In: *Nanoparticle-Based Polymer Composites*. Woodhead Publishing Series

in Composites Science and Engineering. 2022; pp. 15–54. https://doi.org/10.1016/B978-0-12-824272-8.00009-9

11. Jin R, Higaki T. Open questions on the transition between nanoscale and bulk properties of metals. Commun Chem. 2021; 4: 6–9. https://doi.org/10.1038/s42004-021-00466-6
12. Movlarooy T. Study of quantum confinement effects in ZnO nanostructures. Mater Res Express. 2018; 5. https://doi.org/10.1088/2053-1591/aab389
13. Grommet AB, Feller M, Klajn R. Chemical reactivity under nanoconfinement. *Nat* Nanotechnol. 2020; 15: 256–271. https://doi.org/10.1038/s41565-020-0652-2
14. Rizwan M, Ali S, Zia M, Riaz M. Ecotoxicology and Environmental Safety Effects of nanoparticles on trace element uptake and toxicity in plants: A review. 2021; 221. https://doi.org/10.1016/j.ecoenv.2021.112437
15. Wan F, Thakur A, Thakur P. Classification of Nanomaterials (Carbon, Metals, Polymers, Bio-ceramics). In: Suhag, D., Thakur, A., Thakur P (ed). *Integrated Nanomaterials and their Applications*. Springer: Singapore. 2023, 37–55. https://doi.org/10.1007/978-981-99-6105-4_3
16. Sheetal S, Mittal R, Gupta N. Selective synthesis of fluorescent metal nanoclusters over metal nanoparticles. Mikrochim Acta. 2024; 191: 735. https://doi.org/10.1007/s00604-024-06812-4
17. Algar WR, Massey M, Rees K, Higgins R, Krause KD, Darwish GH, Peveler WJ, Xiao Z, Tsai H-Y, Gupta R, Lix K, Tran MV, Kim H. Photoluminescent Nanoparticles for Chemical and Biological Analysis and Imaging. Chem Rev. 2021; 121: 9243–9358. https://doi.org/10.1021/acs.chemrev.0c01176
18. Thomas CD, Hill JK, Hatfield JH. FAR-sighted conservation. 2022;: 1–9. https://doi.org/10.1002/2688-8319.12188
19. Maity S, Das S, Palit M, Dey K, Das B, Kundu T, Paramanik R, De BK, Kunwar HS, Datta S. Electron-magnon coupling mediated magnetotransport in antiferromagnetic van der Waals heterostructures. Phys Rev B - Condens Matter Mater Phys. 2025; 111: L140407. https://doi.org/10.1103/PhysRevB.111.L140407
20. Morris DL. DNA-bound metal ions: recent developments. 2014; 5: 397–407. https://doi.org/10.1515/bmc-2014-0021
21. Mistry L, El-Zubir O, Dura G, Clegg W, Waddell PG, Pope T *et al.* Addressing the properties of "Metallo-DNA" with an Ag(I)-mediated supramolecular duplex. Chem Sci. 2019; 10: 3186–3195. https://doi.org/10.1039/c8sc05103h
22. Petty JT, Zheng J, Hud N V., Dickson RM. DNA-Templated Ag Nanocluster Formation. J Am Chem Soc. 2004; 126: 5207–5212. https://doi.org/10.1021/ja031931o
23. Ijiro K, Mitomo H. Metal nanoarchitecture fabrication using DNA as a biotemplate. Polym J. 2017; 49: 815–824. https://doi.org/10.1038/pj.2017.63
24. Ašanin DP, Bogojevic SS, Perdih F, Andrejević TP, Milivojevic D, Aleksic I *et al.* Structural characterisation, antimicrobial activity and BSA/DNA binding affinity of new silver(I) complexes with thianthrene and 1,8-naphthyridine. Molecules. 2021; 26. https://doi.org/10.3390/molecules26071871
25. Swasey SM, Leal LE, Lopez-Acevedo O, Pavlovich J, Gwinn EG. Silver (I) as DNA glue: Ag(+)-mediated guanine pairing revealed by removing Watson-Crick constraints. Sci Rep. 2015; 5: 10163. https://doi.org/10.1038/srep10163
26. Oyem HH. *Fluorescence Silver Nanoclusters*. 2018; PhD Thesis, Newcastle University, United Kingdom.
27. Dembska A, Świtalska A, Fedoruk-Wyszomirska A, Juskowiak B. Development of fluorescence oligonucleotide probes based on cytosine- and guanine-rich sequences. Sci Rep. 2020; 10: 1–13. https://doi.org/10.1038/s41598-020-67745-5
28. Kretschy N, Sack M, Somoza MM. Sequence-Dependent Fluorescence of Cy3- A nd Cy5-Labeled Double-Stranded DNA. Bioconjug Chem. 2016; 27: 840–848. https://doi.org/10.1021/acs.bioconjchem.6b00053
29. Tevonyan LL, Bazhulia NP, Kaluzhiny DN. Enhancement of intrinsic guanine fluorescence by protonation in DNA of various structures. Biochemie. 2024; 222: 101–108. https://doi.org/10.1016/j.biochi.2024.03.003
30. Barinova IO, Shershov VE, Varachev VO, Surzhikov SA, Grechishnikova IV, Zasedateleva OA, Nasedkina TV, Chudinov AV. Fluorescence Labelling of GC-Rich DNA Matrix with Different Nucleotide Derivatives for Hybridisation Analysis on a Biological Microarray. Russ J Bioorganic Chem. 2025; 51: 1249–1254. https://doi.org/10.1134/S1068162024606918
31. Jia B, Li X, Wang X, Lu Y, Meng H, Zhang X, Wu X, Zhang Z, Deng Y. Investigation on fluorescence enhancement of DNA tetrahedral structures modified DNA-silver nanoclusters for biosensing. Chem EngJ. 2025; 511. https://doi.org/10.1016/j.cej.2025.162251
32. Chen S, Hu W, Cheng Y, Yin Z, Xiao J, Li C, Zhao H, Dong Q, Chen Z. Dimerising DNA-AgNCs via a C–Ag+–C structure for fluorescence sensing with dual-output signals. Chem Commun. 2025; **61**: 2961–2964. https://doi.org/10.1039/D4CC06687A
33. Arakawa H, Ahmad R, Naoui M, Taymir-Riahi H-A. A Comparative Study of Calf Thymus DNA Binding to Cr (III) and Cr (VI) Ions. 2000; 275: 10150–10153. https://doi.org/10.1074/jbc.275.14.10150
34. Shahabadi N, Kashanian S, Ahmadipour Z. DNA binding and gel electrophoresis studies of a new silver(I) complex containing 2,9-dimethyl-1,10-phenanthroline ligands. DNA Cell Biol. 2011; 30: 187–194. https://doi.org/10.1089/dna.2010.1104
35. Neidig ML, Sharma J, Yeh HC, Martinez JS, Conradson SD, Shreve AP. Ag K-edge EXAFS analysis of DNA-templated fluorescent silver nanoclusters: Insight into the structural origins of emission tuning by DNA sequence variations. J Am Chem Soc. 2011; 133: 11837–11839. https://doi.org/10.1021/ja202797w
36. Oyem HH. Binding of Ag (I) ions to DNA nucleobases: A mechanistic study. Nigerian Res Jour of Chem Sci. 2022; 10(2): 31–51.
37. Sletten E. Metal binding to nucleic acids – A journey from the beginning. Inorg Chim Acta. 2016; 452: 273-278. https://doi.org/10.1016/j.ica.2016.02.014
38. Bouhadi M, Javed Q, Jakubus M, Elkouali M, Fougrach H, Ansar A, Goreta BS, Ban D, Heath D, Cerne M. Nanoparticles for Sustainable Agriculture: Assessment of Benefits and Risks. Agronomy. 2025; 15: 1–30. https://doi.org/10.3390/agronomy15051131
39. Paras, YK, Kumar P, Teja DR, Chakraborty S, Chakraborty M, MohapatraSS, Sahoo A, Chou MMC, Liang C-T, Hang D-R. A Review on Low-Dimensional Nanomaterials: Nanofabrication, Characterisation, and Applications. Nanomaterials. 2023; 13: 1–44. https://doi.org/10.3390/nano13010160
40. Hada AM, Lamy de la Chapelle M, Focsan M, Astilean S. Recent Advances in Metal Nanoclusters: From Novel Synthesis to Emerging Applications. Molecules. 2025; 30(19): 3848. https://doi.org/10.3390/molecules30193848
41. Sui M, Kunwar S, Pandey P, Lee J. Strongly confined localised surface plasmon resonance (LSPR) bands of Pt, AgPt, AgAuPt nanoparticles. Sci Rep. 2019; 9: 1–14. https://doi.org/10.1038/s41598-019-53292-1
42. Mcoyi MP, Mpofu KT, Sekhwama M, Mthunzi-Kufa P. Developments in Localised Surface Plasmon Resonance. Plasmonics. 2025; 20: 5481–5520. https://doi.org/10.1007/s11468-024-02620-x
43. Ershov V, Tarasova N, Ershov B. Evolution of electronic state and properties of silver nanoparticles during their formation in aqueous solution. Int J Mol Sci. 2021; 22. https://doi.org/10.3390/ijms221910673
44. Magdy G, Aboelkassim E, Elhaleem SMA, Belal F. A comprehensive review on silver nanoparticles: Synthesis approaches, characterisation techniques, and recent pharmaceutical, environmental, and antimicrobial applications. Microchem J. 2024; 196: 109615. https://doi.org/10.1016/j.microc.2023.109615
45. Ropp RC. Optical and electronic properties of solids. In: *Studies in Inorganic Chemistry*. 2004; 21: 345–446. ScienceDirect, Elsevier. https://doi.org/10.1016/S0169-3158(04)80008-2
46. Strobel EJ. Preparation and characterisation of internally modified DNA templates for chemical transcription roadblocking. Bio-protocol. 2021; 11: 1–42. https://doi.org/10.21769/BioProtoc.4141
47. Fielden SDP. Ostwald Ripening as a Tool for Controlling Dynamic Nanomaterials: Special Collection: 2025 Emerging Investigators. Aggregate. 2025; 6: e70116. https://doi.org/10.1002/agt2.70116Digital Object Identifier (DOI)
48. Alzoubi FY, Ahmad AA, Aljarrah IA, Migdadi AB, Al-Bataineh QM. Localise surface plasmon resonance of silver nanoparticles using Mie theory. J Mater Sci Mater Electron. 2023; 34: 1–10. https://doi.org/10.1007/s10854-023-11304-x
49. Acharya TR, Jang M, Lee GJ, Choi EH. A comprehensive study on the synthesis, characteristics, and catalytic applications of submerged hydrogen-mixed argon plasma-synthesised silver nanoparticles. Curr Appl Phys. 2023; 56: 36–46. https://doi.org/10.1016/j.cap.2023.09.003
50. Kshatriya VV, Kumbhare MR, Jadhav SV, Thorat PJ, Bhambarge RG. Updated Review on Recent Advances in Silver Nanoclusters in Bioanalytical and Biomedical Applications. BIO Integr. 2024; 5: 1–12. https://doi.org/10.15212/bioi-2024-0003

51. Zeiger B. Superatoms. Literature Seminar, Chemistry Department, University of Illinois, USA. 2008.
52. Xie YP, Shen YL, Duan GX, Han J, Zhang LP, Lu X. Silver nanoclusters: Synthesis, structures and photoluminescence. Mater Chem Front. 2020; 4: 2205–2222. https://doi.org/10.1039/D0QM00117A
53. Gombár G, Ungor D, Samu GF, Dömötör O, Csapó E. Synthesis and characterisation of novel blue-emitting nicotinamide-gold nanoclusters with "chain-breaker" antioxidant property. J Mol Liq. 2022; 359: 2–10. https://doi.org/10.1016/j.molliq.2022.119372
54. Ko PK, Ge J, Ding P, Chen D, Tsang HLT, Kumar N, Halpert JE. The Deepest Blue: Major Advances and Challenges in Deep Blue Emitting Quasi-2D and Nanocrystalline Perovskite LEDs. Adv Mater. 2025; 37: 1–31. https://doi.org/10.1002/adma.202407764
55. Nagime P V., Chandak VS. Nanotechnology in Plant-Based Agricultural Innovations. In: Husen A (ed). *Handbook of Nanotechnology in Agriculture*. Springer: Singapore, 2025; 1–35. https://doi.org/10.1007/978-981-96-4489-6_43-1
56. Buceta D, Busto N, Barone G, Leal JM, Domínguez F, Giovanetti LJ, Requejo FG, García B, López-Quintela MA. Ag 2 and Ag 3 Clusters: Synthesis, Characterisation, and Interaction with DNA. Angew Chemie Int Ed. 2015; 54: 7612–7616. https://doi.org/10.1002/anie.201502917
57. Oyem HH, Houlton A, Horrocks BR. Silver nanoclusters prepared in water-in-oil emulsions. Nano Express. 2022; 3. https://doi.org/10.1088/2632-959X/acb83
58. Ledo-Suárez A, Rivas J, Rodríguez-Abreu CF, Rodríguez MJ, Pastor E, Hernández-Creus A *et al.* Facile synthesis of stable subnanosized silver clusters in microemulsions. Angew Chemie - Int Ed. 2007; 46(46): 8823–8827. https://doi.org/10.1002/anie.200702427
59. Copp SM, Schultz DE, Swasey S, Gwinn EG. Atomically precise arrays of fluorescent silver clusters: A modular approach for metal cluster photonics on DNA nanostructures. ACS Nano. 2015; 9(3): 2303–2310. https://doi.org/10.1021/nn506322q
60. Oyem HH. Nanoparticles Synthesis Protocols: A Case of Syntax and Semantics? Ambrose Alli Univ J Phys Appl Sci. 2024; 4: 31–38.
61. Nunn N, Prabhakar N, Reineck P, Magidson V, Kamiya E, Heinz WF, Torelli MD, Rosenholm J, Zaitsev H, Shenderova O. Brilliant Blue, Green, Yellow, and Red Fluorescent Diamond Particles: Synthesis, Characterisation, and Multiplex Imaging Demonstrations. Nanoscale. 2019; 11(24): 11584–11595. https://doi.org/10,1039/c9nr02593f